Surface-Enhanced Raman Scattering on Dendrimer/Metallic Nanoparticle Layer-by-Layer Film Substrates

ARTICLE *in* LANGMUIR · JULY 2005

Impact Factor: 4.46 · DOI: 10.1021/la050202e · Source: PubMed

Surface-Enhanced Raman Scattering on Dendrimer/ Metallic Nanoparticle Layer-by-Layer Film Substrates

Paul J. G. Goulet,† David S. dos Santos, Jr.,† Ramón A. Alvarez-Puebla,† Osvaldo N. Oliveira, Jr.,‡ and Ricardo F. Aroca*,†

Materials & Surface Science Group, School of Physical Sciences, University of Windsor, Windsor, Ontario, Canada N9B 3P4, and Instituto de Física de São Carlos, CP 369, 13560-970 São Carlos, SP, Brazil

Received January 24, 2005. In Final Form: March 27, 2005

In this paper, the fabrication, characterization, and application of unique layer-by-layer (LBL) films of dendrimers and metallic nanoparticles is reported. Silver nanoparticles (d = ∼20 nm) are produced in solution by sodium citrate reduction and incorporated into thin films with generation 1 and 5 DAB−Am dendrimers (polypropylenimine dendrimers with amino surface groups) by the LBL technique. The resulting nanocomposite films are characterized by UV−visible surface plasmon absorption and atomic force microscopy (AFM) measurements, and employed as substrates for surface-enhanced Raman scattering (SERS) of 2-naphthalenethiol. Through variation of the molecular size (dendrimer generation) and concentration of the cross-linker used, as well as the number of layers produced, the optical properties of several different possible architectures are studied. In the films, Ag nanoparticles are shown to be effectively immobilized and stabilized with increased control over their spacing and aggregation. Moreover, the films are shown to be excellent substrates for SERS measurements, demonstrating significant enhancement capability. As expected, large electromagnetic enhancement of Raman scattering signals is found to be strongly dependent on interparticle coupling between neighboring metallic nanoparticles. Finally, the possibility of detecting SERS signals from architectures with intervening layers between the metal nanoparticles and analyte molecules is explored. It is shown that although there are decreases in intensity with increasing number of intervening layers (as is expected from the distance dependence of SERS), electromagnetic enhancement is still able to function at these distances, thus offering the possibility of developing sensors with external layers that are chemically selective for specific analytes.

Introduction

Surface-enhanced Raman scattering (SERS) is a phenomenon involving large increases in Raman scattering cross sections of molecules adsorbed at the surfaces of nanometric-scale metallic particles.[1−4] Since its first observation in 1974,[5] SERS has been an object of great scientific interest and has led to advancement in the study of many related topics, particularly the optical properties of metallic nanoparticles.[6−10] More recently it has begun to be employed increasingly toward microanalytical applications in a wide variety of fields.[11−15] In particular, the high spatial resolution,[16,17] ultrasensitivity,[18−20] and high information content[21−23] provided by SERS make it an especially powerful technique. These strengths have now been employed by several groups to demonstrate detection and spectroscopic identification of analytes down to the single molecule level.[24−30] The metallic nanostructured substrates that are used for SERS measurements are able to sustain dipole particle plasmon resonances

* Corresponding author: e-mail raroca1@cogeco.ca.
† University of Windsor.
‡ Instituto de Física de São Carlos.

(1) Moskovits, M. *Rev. Mod. Phys.* **1985**, *57*, 783.
(2) Metiu, H. *Prog. Surf. Sci.* **1984**, *17*, 153−320.
(3) Chang, R. K., Furtak, T. E., Eds. *Surface Enhanced Raman Scattering*; Plenum Press: New York, 1982.
(4) Vo-Dinh, T. *TrAC, Trends Anal. Chem.* **1998**, *17*, 557−582.
(5) Fleischmann, M.; Hendra, P. J.; McQuillan, A. J. *Chem. Phys. Lett.* **1974**, *26*, 163−166.
(6) Schatz, G. C.; Van Duyne, R. P. In *Handbook of Vibrational Spectroscopy*; Chalmers, J. M., Griffiths, P. R., Eds.; John Wiley & Sons: Ltd.: Chichester, UK, 2002; Vol. 1, pp 759−774.
(7) Barber, P. W.; Chang, R. K.; Massoudi, H. *Phys. Rev. B* **1983**, *27*, 7251−7261.
(8) Eagen, C. F. *Appl. Opt.* **1981**, *20*, 3035−3042.
(9) Etchegoin, P.; Cohen, L. F.; Hartigan, H.; Brown, R. J. C.; Milton, M. J. T.; Gallop, J. C. *J. Chem. Phys.* **2003**, *119*, 5281−5289.
(10) Gresillon, S.; Aigouy, L.; Boccara, A. C.; Rivoal, J. C.; Quelin, X.; Desmarest, C.; Gadenne, P.; Shubin, V. A.; Sarychev, A. K.; Shalaev, V. M. *Phys. Rev. Lett.* **1999**, *82*, 4520−4523.
(11) Cao, Y. C.; Jin, R.; Mirkin, C. A. *Science* **2002**, *297*, 1536−1540.
(12) Moore, B. D.; Stevenson, L.; Watt, A.; Flitsch, S.; Turner, N. J.; Cassidy, C.; Graham, D. *Nat. Biotechnol.* **2004**, *22*, 1133−1138.
(13) Kneipp, K.; Kneipp, H.; Itzkan, I.; Dasari, R. R.; Feld, M. S. *Curr. Sci.* **1999**, *77*, 915−926.
(14) Jarvis, R. M.; Goodacre, R. *Anal. Chem.* **2004**, *76*, 40−47.
(15) Culha, M.; Stokes, D. L.; Allain, L. R.; Vo-Dinh, T. *Anal. Chem.* **2003**, *75*, 6196−6201.
(16) Deckert, V.; Zeisel, D.; Zenobi, R.; Vo-Dinh, T. *Anal. Chem.* **1998**, *70*, 2646−2650.
(17) Pettinger, B.; Ren, B.; Picardi, G.; Schuster, R.; Ertl, G. *Phys. Rev. Lett.* **2004**, *92*, 096101−096101−096101−096104.
(18) Hildebrandt, P.; Stockburger, M. *J. Phys. Chem.* **1984**, *88*, 5935−5944.
(19) Kneipp, K.; Kneipp, H.; Itzkan, I.; Dasari, R. R.; Feld, M. S. *Chem. Rev.* **1999**, *99*, 2957−.
(20) Constantino, C. J. L.; Lemma, T.; Antunes, P. A.; Aroca, R. F. *Anal. Chem.* **2001**, *73*, 3674−3678.
(21) Long, D. A. *The Raman Effect: A Unified Treatment of the Theory of Raman Scattering by Molecules*; John Wiley & Sons: Ltd.: Chichester, UK, 2002.
(22) Jennings, C.; Kovacs, G. J.; Aroca, R. F. *Langmuir* **1993**, *9*, 2151−2155.
(23) Goulet, P. J. G.; Aroca, R. F. *Can. J. Chem.* **2004**, *82*, 987−997.
(24) Kneipp, K.; Wang, Y.; Kneipp, H.; T. Perelman, L. T.; Itzkan, I. *Phys. Rev. Lett.* **1997**, *78*, 1667−1670.
(25) Nie, S.; Emory, S. R. *Science* **1997**, *275*, 1102−1106.
(26) Xu, H.; Bjerneld, E. J.; Kall, M.; Borjesson, L. *Phys. Rev. Lett.* **1999**, *83*, 4357−4360.
(27) Michaels, A. M.; Nirmal, M.; Brus, L. E. *J. Am. Chem. Soc.* **1999**, *121*, 9932−9939.
(28) Moskovits, M.; Tay, L. L.; Yang, J.; Haslett, T. L. In *Optical Properties of Nanostructured Random Media*; Shalaev, V. M., Ed.; Springer-Verlag: Berlin Heidelberg, 2002, pp 215−226.
(29) Maher, R. C.; Cohen, L. F.; Etchegoin, P. *Chem. Phys. Lett.* **2002**, *352*, 378−384.
(30) Goulet, P. J. G.; Pieczonka, N. P. W.; Aroca, R. F. *Anal. Chem.* **2003**, *75*, 1918−1923.

10.1021/la050202e CCC: $30.25
Published on Web 04/27/2005

(generally in the visible region of the spectrum), which lead to large local electromagnetic fields at their surfaces.[31] These substrates have been fabricated by a variety of physical and chemical methods, producing a wide assortment of interesting architectures.[32−39] Some of these architectures include those produced by vacuum evaporation of metal,[39−41] electrochemical roughening of metal electrodes,[42,43] and lithographical techniques.[34,44] However, the use of these techniques tends to be somewhat limited because they require expensive specialized equipment or specialized techniques. Chemically reduced colloidal metal solutions, on the other hand, are quite easy to prepare and have now become the most widely used SERS substrates.[45,46]

Despite the exceptional utility that these colloidal solutions have shown as SERS substrates, there are some drawbacks to their use. First and foremost, they can become very unstable and collapse with the introduction of analyte molecules, due to a reduction in the repulsive forces between the particles. In addition, when working in solution, fairly strong adsorption of molecules onto particles, producing short interaction distances, is required for large enhancement, but this may not exist for all combinations of interest. Finally, when these solutions are cast onto solid surfaces, we severely lack control over the resulting interparticle spacing. It is known, however, that this spacing critically determines the optical properties of the aggregates produced, including the large electromagnetic fields that define SERS. One simple method for SERS substrate fabrication that seems to address all of these issues is the layer-by-layer (LBL) technique.

The layer-by-layer technique was pioneered by Decher[47] and involves the electrostatic assembly of alternating positively and negatively charged layers. It is an extremely versatile method for nanodimension film fabrication, and this can be seen in the large variety of materials that have been employed in LBL films.[48] These supramolecular architectures may be tailored for specific applications, including those in biology, optics, and electronics.[49,50] Included in the materials that are particularly well suited for use in LBL films are dendrimers.[51] These are macromolecules composed of a core (generation zero) and a hyperbranched structure that extends in a highly organized fashion out to the terminal groups. In contrast to conventional polymers, dendrimers have precisely controlled structures, molecular weights, and chemical functionalities. They have recently been employed as stabilizers in the synthesis of metallic nanoparticles of gold and silver, with reducing agents such as borohydrate and citrate.[52−54] In some cases, dendrimers have been applied directly as reducing agents for the production of metallic nanoparticles.[55]

Several groups have now begun to incorporate metallic nanoparticles into LBL thin films[56−58] and to examine the use of these films as substrates for SERS measurements.[59,60] In this work, we utilize the exceptional characteristics of dendrimers along with the powerful optical properties of colloidal Ag nanospheres to produce unique SERS substrates by the LBL self-assembly technique. Films are prepared by successive alternating immersions in solutions of dendrimer and colloidal Ag particles and characterized by surface plasmon absorption and atomic force microscopy. They are shown to provide excellent enhancement of the Raman scattering of 2-naphthalenethiol. The optical properties of several different possible architectures are studied as a function of the size (generation) and concentration of the dendrimer used, as well as the number of layers produced. Ag nanoparticles are shown to be effectively immobilized and stabilized by the dendrimers, with increased control over their spacing and aggregation. Finally, the possibility of collecting SERS from architectures with intervening layers between metal nanoparticles and analyte molecules is demonstrated.

Experimental Section

All glassware was thoroughly cleaned with water, aqua regia, and then deionized water. Glass microscope slides were cleaned prior to LBL film deposition by employing Kern's method.[61] Colloidal silver solutions were obtained by citrate reduction of $AgNO_3$ according to the method proposed by Lee and Meisel[45] and used as synthesized. Solutions of generation 5 DAB−Am-64 poly(propylenimine tetrahexacontaamine) dendrimer (Aldrich), 1.0 g/L; generation 2 DAB−Am-8 poly(propylenimine octaamine) dendrimer, (Aldrich), 2.4 and 1.0 g/L; and poly(styrene sulfonate), PSS (Aldrich), 1.0 g/L, in Milli-Q water (18.2 MΩ cm), were also prepared and used in the fabrication of the LBL multilayer films. All films were prepared by immersing clean glass substrates into dendrimer solutions for 10 min (allowing for interaction of the protonated amines of the dendrimer with the acidic OH groups of the glass surface), rinsing them with Milli-Q water, drying them with nitrogen gas, and then immersing

(31) Kelly, K. L.; Coronado, E.; Zhao, L. L.; Schatz, G. C. *J. Phys. Chem. B* **2003**, *107*, 668−677.
(32) Wu, Y.; Livneh, T.; Zhang, Y. X.; Cheng, G.; Wang, J.; Tang, J.; Moskovits, M.; Stucky, G. D. *Nano Lett.* **2004**, *4*, 2337−2342.
(33) dos Santos, D. S., Jr.; Goulet, P. J. G.; Pieczonka, N. P. W.; Oliveira, O. N., Jr.; Aroca, R. F. *Langmuir* **2004**, *20*, 10273−10277.
(34) Green, M.; Liu, F. M. *J. Phys. Chem. B* **2003**, *107*, 13015−13021.
(35) Chan, S.; Kwon, S.; Koo, T.-W.; Lee, L. P.; Berlin, A. A. *Adv. Mater.* **2003**, *15*, 1595−1598.
(36) Bjerneld, E. J.; Svedberg, F.; Kaell, M. *Nano Lett.* **2003**, *3*, 593−596.
(37) Freeman, R. G.; Grabar, K. C.; Allison, K. J.; Bright, R. M.; Davis, J. A.; Guthrie, A. P.; Hommer, M. B.; Jackson, M. A.; Smith, P. C.; Walter, D. G.; Natan, M. J. *Science* **1995**, *267*, 1629−1632.
(38) Tao, A.; Kim, F.; Hess, C.; Goldberger, J.; He, R.; Sun, Y.; Xia, Y.; Yang, P. *Nano Lett.* **2003**, *3*, 1229−1233.
(39) Brolo, A.; Arctander, E.; Gordon, R.; Leathem, B.; Kavanagh, K. L. *Nano Lett.* **2004**, *4*, 2015−2018.
(40) Semin, D. J.; Rowlen, K. L. *Anal. Chem.* **1994**, *66*, 4324−4331.
(41) Schlegel, V. L.; Cotton, T. M. *Anal. Chem.* **1991**, *63*, 241−247.
(42) Albrecht, M. G.; Creighton, J. A. *J. Am. Chem. Soc.* **1977**, *99*, 5215−5217.
(43) Ren, B.; Lin, X.-F.; Yang, Z.-L.; Liu, G.-K.; Aroca, R. F.; Mao, B. W.; Tian, Z. Q. *J. Am. Chem. Soc.* **2003**, *125*, 9598−9599.
(44) Liao, P. F.; Bergman, J. G.; Chemla, D. S.; Wokaun, A.; Melngailis, J.; Hawryluk, A. M.; Economou, N. P. *Chem. Phys. Lett.* **1981**, *82*, 355−359.
(45) Lee, P. C.; Meisel, D. *J. Phys. Chem.* **1982**, *86*, 3391−3395.
(46) Sanchez-Cortes, S.; Garcia-Ramos, J. V.; Morcillo, G. *J. Coll. Int. Sci.* **1994**, *167*, 428−436.
(47) Decher, G. *Science* **1997**, *277*, 1232−1237.
(48) Raposo, M.; Oliveira, O. N., Jr. *Braz. J. Phys.* **1998**, *28*, 392−404.
(49) Zucolotto, V.; Barbosa Neto, N. M.; Rodrigues, J. J., Jr.; Constantino, C. J. L.; Zilio, S. C.; Mendonca, C. R.; Aroca, R. F.; Oliveira, O. N., Jr. *J. Nanosci. Nanotechno.* **2004**, *4*, 855−860.
(50) Liu, H.; Rusling, J. F.; Hu, N. *Langmuir* **2004**, *20*, 10700−10705.
(51) Tomalia, D. A.; Naylor, A. M.; Goddard, W. A. *Angew. Chem., Int. Ed.* **1990**, *29*, 138−175.
(52) Esumi, K.; Suzuki, A.; Yamahira, A.; Torigoe, K. *Langmuir* **2000**, *16*, 2604−2608.
(53) Manna, A.; Imae, T.; Aoi, K.; Okada, M.; Yogo, T. *Chem. Mater.* **2001**, *13*, 1674−1681.
(54) Musick, M. D.; Keating, C. D.; Lyon, L. A.; Botsko, S. L.; Pena, D. J.; Holliway, W. D.; McEvoy, T. M.; Richardson, J. N.; Natan, M. J. *Chem. Mater.* **2000**, *12*, 2869−2881.
(55) Esumi, K.; Hosoya, T.; Suzuki, A.; Torigoe, K. *J. Coll. Int. Sci.* **2000**, *226*, 346−352.
(56) Schneider, G.; Decher, G. *Nano Lett.* **2004**, *4*, 1833−1839.
(57) Tian, S.; Liu, J.; Zhu, T.; Knoll, W. *Chem. Mater.* **2004**, *16*, 4103−4108.
(58) Salgueirino-Maceira, V.; Caruso, F.; Liz-Marzan, L. M. *J. Phys. Chem. B* **2003**, *107*, 10990−10994.
(59) Aroca, R. F.; Goulet, P. J. G.; dos Santos, D. S., Jr.; Alvarez-Puebla, R. A.; Oliveira, O. N., Jr. *Anal. Chem.* **2005**, *77*, 378−382.
(60) Li, X.; Xu, W.; Zhang, J.; Jia, H.; Yang, B.; Zhao, B.; Li, B.; Ozaki, Y. *Langmuir* **2004**, *20*, 1298−1304.
(61) Kern, W. *Semicond. Int.* **1984**, *94*, 94−98.

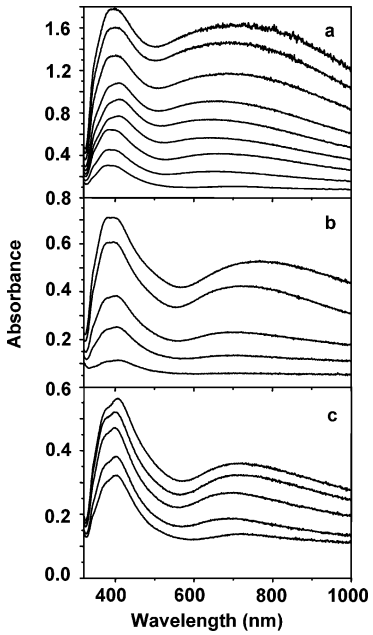

Figure 1. UV−visible absorption spectra of layer-by-layer films showing increasing extinction with increasing number of bilayers for films produced with a Ag nanosphere solution and (a) generation 5 DAB−Am dendrimer solution (1.0 g/L) (up to 9 bilayers), (b) generation 1 DAB−Am dendrimer solution (2.4 g/L) (up to 5 bilayers), and (c) generation 1 DAB−Am dendrimer solution (1.0 g/L) (up to 5 bilayers). Increasing number of bilayers correlates in all cases with increased extinction.

them into solutions containing silver nanospheres for 2 h. Upon completion of these steps, the films were rinsed and dried and could be then be used for the possible deposition of further dendrimer/nanosphere bilayers. Importantly, the colloidal silver solution was changed after each deposition. In the cases where PSS spacer layers were substituted for Ag nanosphere layers, they were deposited by the same procedures but with immersion times of only 10 min for each layer.

To monitor their surface plasmon absorption, UV−visible absorption spectra were obtained for all colloidal solutions and nanocomposite films produced, on a Cary 50 UV−visible spectrometer. Atomic force microscopy (AFM) measurements were performed on a Digital Instruments NanoScope IV operating in noncontact tapping mode with a n^+-silicon tip (NSC 14 model, Ultrasharp) operating at a resonant frequency of 256 kHz. All images were collected with high resolution (512 lines with 512 samples/line) at a scan rate of 0.5 Hz. The data were collected under ambient conditions, and each scan was duplicated to ensure that any features observed were reproducible. Raman scattering experiments were conducted by employing a micro-Raman Renishaw InVia system with laser excitation at 785 nm (diode laser) directed through a 5× microscope objective and focused to an area of $\sim 10\ \mu m^2$. Laser power at the sample was 2.5 mW, and 10 s spectral accumulation times were employed. All samples for SERS measurements were prepared by casting 30 μL of a 10^{-3} M ethanol solution of 2-naphthalenethiol, NFT (Aldrich), onto the LBL film substrates and allowing the solvent to evaporate.

Results and Discussion

Layer-by-layer film depositions, as well as the properties of films produced by this technique, are known to depend critically upon the various experimental parameters employed. Among the most important of these are the chemistry, size, and concentration of the species involved and the number of deposition steps performed. In this work, an attempt has been made to systematically study these variables for LBL films produced from colloidal Ag and DAB−Am dendrimer (polypropylenimine dendrimers with amino surface groups) solutions. In Figure 1, the growth of films is monitored by UV−visible absorption spectroscopy for generation 5 and generation 1 DAB−Am dendrimer/Ag multilayers. The surface plasmon absorption spectra for LBL films produced with a 1.0 g/L generation 5 DAB−Am dendrimer solution as the source of the cationic species are shown in Figure 1a, while the spectra for films produced from 2.4 and 1.0 g/L solutions of generation 1 DAB−Am dendrimer are shown in Figure 1, panels b and c, respectively.

There are several traits that appear to be common to all three sets of experiments. First, the overall shape of the absorption spectra is similar for all films, displaying a broad maximum at ∼390 nm and a second broad feature at ∼700 nm. The former can be largely attributed to the absorption of single isolated Ag particles with a mean diameter of ∼20 nm but also appears to have contributions from the transverse plasmon mode of coupling particles. The latter feature, on the other hand, is the result of the absorption due to coupling particles, whether as dimers or higher order aggregates. The 390 nm band observed for the films is blue-shifted by 18 nm relative to the Ag citrate colloidal solution (results not shown), and this can be explained by the reduction in the index of refraction of the surrounding medium (water to air) and by the added contribution to this band of the transverse plasmon mode of coupling particles. Second, in all three cases, the extinction of the films grows with the addition of each bilayer, indicating that, within these limits, adsorption of the nanoparticles is a favored process over desorption. Finally, in all three sets of spectra, a general trend toward growth in the relative intensity of the longer wavelength band is observed with increasing number of bilayers, before stabilizing after ∼3 bilayers have been deposited. This can be interpreted as an increase in the number of electromagnetically coupling nanoparticles relative to single isolated ones, and ultimately to the uneven distribution of material in the initial bilayers.

By comparing the corresponding data of Figure 1 panels a and c, it can be seen that higher Ag adsorption occurs with the generation 5 dendrimer than with the generation 1 dendrimer (with equal concentrations of 1.0 g/L), as revealed by higher surface plasmon absorption. This suggests that there are a larger number of available amino groups for binding Ag nanoparticles on the surface of the generation 5 dendrimer films than on the generation 1 films. This also holds when the concentration of the generation 1 dendrimer is increased to 2.4 g/L, as in Figure 1b. Moreover, a comparison of the spectra in Figure 1 panels b and c reveals that the higher concentration of generation 1 dendrimer also leads to increased adsorption of silver nanoparticles, and thus higher absorption. It was also found that the adsorption of Ag nanoparticles on the dendrimer layers continued to increase up to 20 h (results not shown here), likely indicating that film growth is not governed by strong electrostatic interactions alone and that other driving forces such as van der Waals or hydrogen-bond interactions may also play an important role.[62]

The surface morphologies of the LBL films produced in this work were analyzed by AFM imaging. The results obtained for films prepared from a generation 5 dendrimer solution with a concentration of 1.0 g/L and a Ag colloidal solution are shown in Figure 2. These images are of the films produced with 1−6 bilayers and correspond to the lower six absorption spectra of Figure 1a. On the basis of the analysis of these images, the mean diameter of the silver nanoparticles was found to be ∼20 nm. With the

(62) Raposo, M.; Pontes, R. S.; Mattoso, L. H. C.; Oliveira, O. N., Jr. *Macromolecules* **1997**, *30*, 6095−6101.

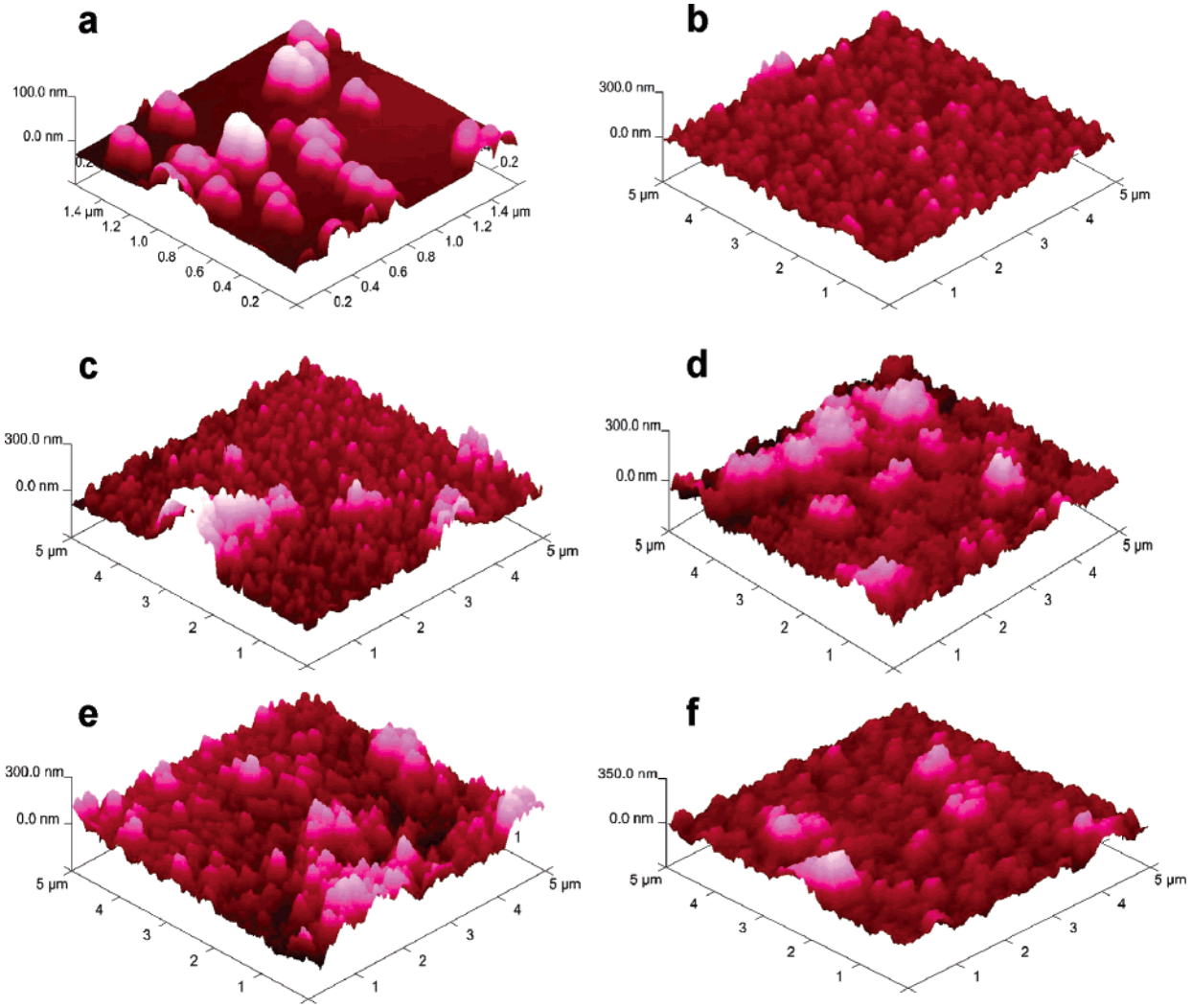

Figure 2. AFM images recorded from layer-by-layer films with alternating layers of Ag nanospheres and generation 5 DAB−Am dendrimer (1.0 g/L), demonstrating the effect of increasing number of bilayers on film morphology and RMS roughness: (a) 1 bilayer (RMS = 20.2 nm), (b) 2 bilayers (RMS = 40.2 nm), (c) 3 bilayers (RMS = 55.3 nm), (d) 4 bilayers (RMS = 63.1 nm), (e) 5 bilayers (RMS = 67.0 nm), and (f) 6 bilayers (RMS = 62.9 nm).

deposition of a single bilayer, the vast majority of nanoparticles are observed as single isolated particles or as dimers, with the surface being covered quite incompletely, as shown in Figure 2a. This effect is commonly observed for LBL films and is the result of the nonuniform coverage of the glass substrate by the first dendrimer layer. As the number of bilayers deposited is increased up to 6, as shown in Figure 2b−f, however, surface coverage becomes more complete, forming continuous interacting networks of nanoparticles with occasional larger aggregates. The RMS roughness values of the films also seem to support the notion that after the first few bilayers have been deposited, the depositions become more consistent and the surface morphology changes little with each additional bilayer. The first bilayer has an RMS roughness value of ~20 nm, and this is fairly consistent with the mean particle size. As more layers are added to the film, the roughness of the surface increases up to approximately 60 nm in the third layer, after which it remains relatively constant with increasing numbers of bilayers.

In Figure 3, the effect of the number of bilayers of generation 5 dendrimers and Ag nanoparticles on the SERS intensity of 2-naphthalenethiol cast onto LBL film substrates is examined. In Figure 3a, the SERS spectrum obtained directly from a bare generation 5 DAB−Am dendrimer/Ag LBL film (1 bilayer) is shown. It is consistent with the Raman spectrum of the dendrimer alone and is of relatively low intensity. As a reference for the SERS spectra reported here, the normal Raman scattering spectrum of 2-naphthalenethiol powder is shown in Figure 3b. This spectrum, along with the SERS spectrum of this molecule, has been reported previously.[63] The SERS spectra of 2-naphthalenethiol cast onto LBL films of 1−6 bilayers are shown in Figures 3c−h and were all recorded under the same experimental conditions with a 785 nm diode laser. The SERS spectra recorded from all the substrates show the same basic features, with nearly no variation in the relative intensities, frequencies, or bandwidths of the observed bands. However, there is an important trend revealed in the total observed average intensities of the spectra, and this is illustrated by the numbers in parentheses for each of the SERS spectra in Figure 3, which indicate the intensity of the 1382 cm^{-1} band of 2-naphthalenethiol in kilocounts. Notably, these numbers are not SERS enhancement factors; they are simply a direct comparison of observed signals, under identical experimental conditions, in kilocounts. It can be seen, however, that average enhancement increases,

(63) Alvarez-Puebla, R. A.; dos Santos, D. S., Jr.; Aroca, R. F. *Analyst* **2004**, *129*, 1251−1256.

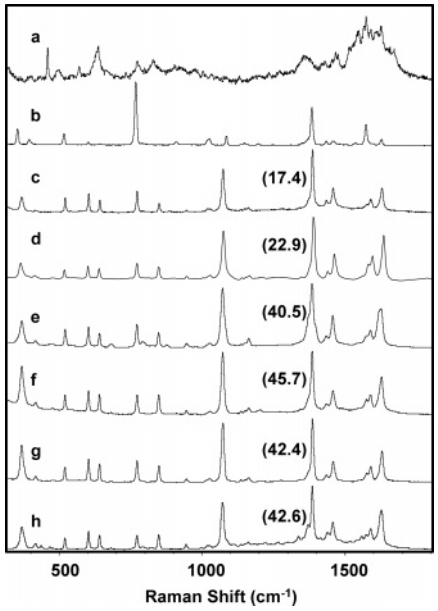

Figure 3. (a) SERS spectrum of a bare generation 5 DAB−Am dendrimer/Ag LBL film (1 bilayer). (b) Normal Raman scattering spectrum of 2-naphthalenethiol powder. Also shown are the SERS spectra recorded from 2-naphthalenethiol cast onto LBL films, fabricated from Ag nanospheres and generation 5 DAB−Am dendrimer, and composed of (c) 1, (d) 2, (e) 3, (f) 4, (g) 5, and (h) 6 bilayers. The number in parentheses for each spectrum indicates the average intensity of the 1382 cm^{-1} band of 2-naphthalenethiol in kilocounts, where all spectra were recorded under the same experimental conditions.

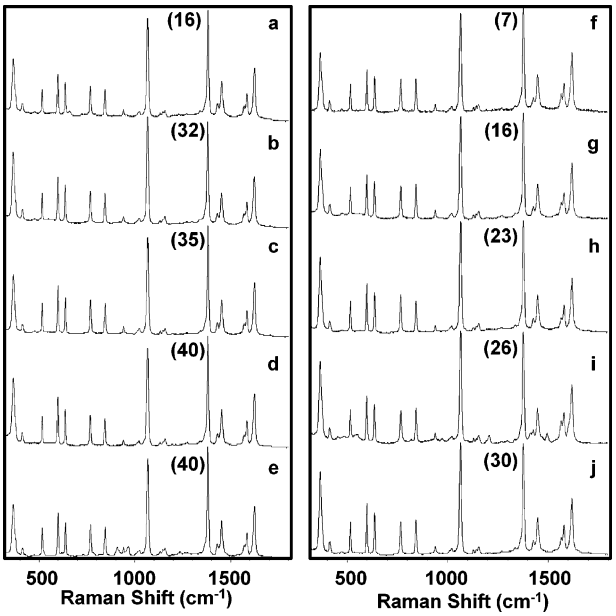

Figure 4. Comparison of SERS spectra of 2-naphthalenethiol as a function of the concentration of generation 1 DAB−Am dendrimer used to produce the LBL substrates, and the number of bilayers they are composed of. All spectra on the left (a−e) were produced from a 2.4 g/L generation 1 solution, and are composed of (a) 1, (b) 2, (c) 3, (d) 4, and (e) 5 bilayers. All spectra on the right (f−j), however, were produced from a 1.0 g/L generation 1 solution, and are composed of (f) 1, (g) 2, (h) 3, (i) 4, and (j) 5 bilayers. The number in parentheses for each spectrum indicates the average intensity of the 1382 cm^{-1} band of 2-naphthalenethiol in kilocounts, where all spectra were recorded under the same experimental conditions.

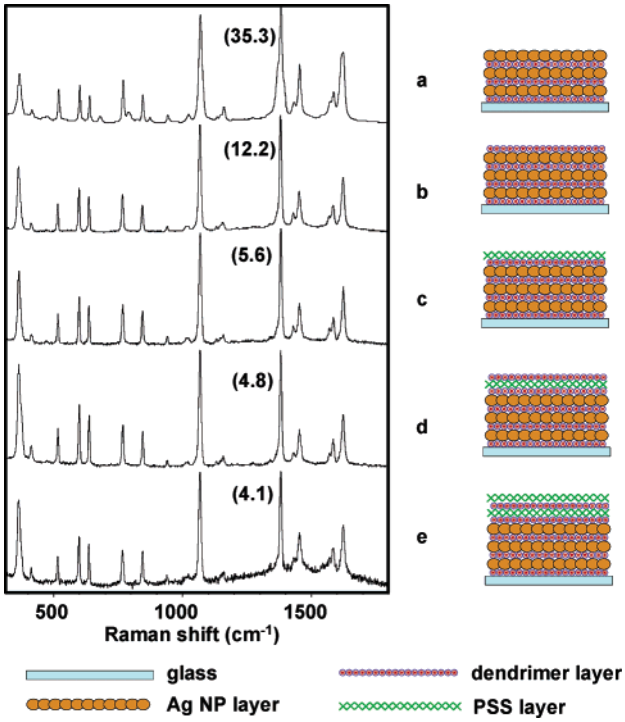

Figure 5. SERS spectra from LBL substrates demonstrating the effect on intensity of introducing intervening layers between the Ag nanospheres and the 2-naphthalenethiol analyte molecules. Films were prepared from colloidal Ag, 1.0 g/L generation 5 DAB−Am dendrimer, and 1 g/L polystyrene sulfonate (PSS) solutions, and SERS spectra were recorded from evaporated solutions of 2-naphthalenethiol cast onto them. The number in parentheses for each spectrum indicates the average intensity of the 1382 cm^{-1} band of 2-naphthalenethiol in kilocounts, where all spectra were recorded under the same experimental conditions. The architectures are (a) 3 dendrimer/Ag bilayers, (b) 3.5 dendrimer/Ag bilayers, (c) 3 dendrimer/Ag bilayers + 1 dendrimer/PSS bilayer, (d) 3 dendrimer/Ag bilayers + 1.5 dendrimer/PSS bilayers, and (e) 3 dendrimer/Ag bilayers + 2 dendrimer/PSS bilayers, as shown in the legend.

proceeding from 1 to 3 generation 5 dendrimer/Ag bilayers, before stabilizing. This trend is likely the result of increased surface coverage, surface area, and aggregation (larger numbers of structures resonant at 785 nm) with increasing numbers of bilayers and agrees well with the trends observed for surface plasmon absorption and AFM measurements.

Strong SERS enhancement can also be observed from 2-naphthalenethiol cast onto LBL film substrates prepared from generation 1 dendrimer and Ag nanoparticle solutions, as shown in Figure 4. In this figure, the effect of concentration of the cationic dendrimer species on the average enhancement of the SERS signals collected from the substrates is explored. In agreement with the surface plasmon absorption results presented for these film sets, the average enhancement of the Raman scattering signals is significantly higher for the films prepared with the higher dendrimer concentration (spectra a−e). This is likely due to higher concentrations of nanostructures resonant at 785 nm and also possibly to increases in electromagnetic fields surrounding the nanostructures due to higher particle−particle coupling in these films. In addition, these substrate sets seem to show similar behavior to those prepared from the generation 5 dendrimer (Figure 3), as enhancement grows initially when bilayers are added and then stabilizes.

In all the SERS experiments described above, enhancement was observed for the Raman scattering signals of

analytes deposited directly onto Ag nanoparticle layers. To demonstrate that it may also be possible to develop sensors with external layers that are chemically selective for specific analytes without significantly decreasing the enhancement afforded by SERS, experiments have been performed with architectures having intervening spacer layers between the metal nanoparticles and analyte molecules. These architectures were prepared by substituting outer Ag nanoparticle layers with the polymer poly(styrene sulfonate) (PSS), as shown in Figure 5. Although there are decreases in average SERS intensities with increasing numbers of intervening layers, as is expected from the distance dependence of SERS and confirmed in Figure 5, electromagnetic enhancement is still strong, even with two complete spacer layers between the metallic nanoparticles and analyte molecules.

Conclusions

In this work, the layer-by-layer technique was successfully employed in the production of unique substrates for measurements of surface-enhanced Raman scattering. The exceptional characteristics of dendrimers along with the powerful optical properties of colloidal Ag nanospheres were utilized to produce a variety of different film architectures, and these were studied by surface plasmon absorption, AFM, and SERS measurements. It was shown that the optical properties of these different substrate architectures are strongly influenced by the generation and concentration of the dendrimers used, as well as the number of layers produced. These LBL films were shown to have some particular benefits over many commonly used substrates for SERS and were able to provide excellent enhancement of the Raman scattering of 2-naphthalenethiol. Finally, the collection of SERS from architectures with spacer layers between the metal nanoparticles and analyte molecules was demonstrated, showing potential for application in the development of chemically specific SERS sensors.

Acknowledgment. Financial assistance from NSERC of Canada and from CNPq and FAPESP of Brazil is gratefully acknowledged.

LA050202E